united nations
educational, scientific
and cultural
organization

international atomic
energy agency

the
abdus salam
international centre for theoretical physics

H4.SMR/1519-36

"Seventh Workshop on Non-Linear Dynamics and Earthquake Prediction"

29 September - 11 October 2003

Seismological Observations on the Interaction between the Brittle and Ductile Part of the Lithosphere

Keiiti AKI

Observatoire Volcanologique
14 Route Nationale 3
971418, La Plaine des Cafres, La Reunion
France

Temporal (un)correlations between coda Q and seismicity — multiscale trend analysis

I. Zaliapin [*], A. Jin [†], Z. Liu [‡], K. Aki [§] and V. Keilis-Borok [¶]

September 10, 2003

[*]Institute of Geophysics and Planetary Physics, University of California, Los Angeles, USA, 90095-1567, and International Institute of Earthquake Prediction Theory and Mathematical Geophysics, Russian Academy of Sciences, Moscow, Russia, E-mail: zal@ess.ucla.edu Phone: +10-310-8256115, Fax: +10-310-2063051, corresponding author.

[†]Association for the Development of Earthquake Prediction, Tokyo, 101-0064, Japan; National Research Institute for Earth Sciences and Disaster Prevention, Tsukuba, Ibaraki 300-0006, Japan. E-mail: ajin@bosai.go.jp

[‡]Department of Earth and Space Sciences, University of California, Los Angeles, USA, E-mail: zliu@ess.ucla.edu

[§]Observatoire Volcanologique du Piton de la Fournaise, La Plaine des Cafres, France, E-mail: aki@ipgp.jussieu.fr

[¶]Department of Earth and Space Sciences and Institute of Geophysics and Planetary Physics, University of California, Los Angeles, USA, E-mail: vkb@ess.ucla.edu

Abstract

This paper introduces a statistical technique, based on the recently developed Multiscale Trend Analysis (MTA), for quantifying correlations between non-stationary processes observed at irregular non-coincident time grids. We apply this technique to studying the temporal correlation between the dynamics of the ductile and brittle layers in the lithosphere. Our results confirm the previously reported strong positive correlation between the coda Q^{-1} and seismicity and its drop before major earthquakes observed in California. The proposed technique has significant advantages over the conventional correlation analysis: (1) MTA allows one to work directly with non-coincident time series without preliminary resampling the data; (2) The correlation is defined via the stable objects — trends — rather than noisy individual observations, hence it is highly robust; (3) The correlations are quantified at different time scales. The suggested technique seems promising for the wide range of applied problems dealing with coupled time series.

Running title: Multiscale analysis of brittle-ductile correlation

Key words: Brittle-ductile correlation, multiscale trend analysis

1 Introduction

Temporal correlations between the coda Q^{-1} and seismicity have been reported for seismic regions worldwide (CHOUET, 1979; AKI, 1985; JIN AND AKI, 1986, ROBINSON, 1987, TSUKUDA, 1988; SATO, 1988) although, the patterns of these correlations vary significantly from case to case. Throughout a systematic measurements on the coda Q^{-1} and seismicity in California for over 50 years, JIN AND AKI (1989, 1993) and AKI (1996) demonstrated that all the collected observations may be interpreted in terms of strong positive correlations between the temporal variation in Q^{-1} and the fractional rate $N(M_c)$ of earthquakes with magnitude M_c, characteristic to a seismic region. Based on these findings, JIN AND AKI (1989,1993) proposed the "Creep model" assuming the presence of ductile fractures in the brittle-ductile transition zone with a unique scale length characteristic to a seismic region. The increase in fractures in the ductile part increases coda Q^{-1} and, at the same time, generates stress concentration with the same scale length responsible for the increase in frequency of earthquakes around magnitude M_c. The scale length corresponding to the observed M_c is a few hundred meters for Southern California and roughly 1 km for Central California. When the stress in the brittle part builds up over time to the point of failure preparing for a major earthquake, we may expect a change in its mechanical property as a whole as suggested in various laboratory experiments on rock samples. We then expect a switch in the mode of loading and, as a consequence, the break down of the positive simultaneous correlation between coda Q^{-1} and $N(M_c)$. That is exactly what was found by JIN et al. (2003) for several years prior to the M7.1 Loma Prieta earthquake of 1989 and for several years prior to the M7.3 Kern County earthquake of 1952.

According to the aforementioned observations together with what has been learnt from the quantitative prediction of the volcanic eruptions at Piton de la Fournaise the creep model was recently revised by AKI (2003, 2003a) as the "Brittle-Ductile interaction hypothesis". It states that the correlation between Q^{-1} and $N(M_c)$ may be an indicator of the regional earthquake cycle: it is positive and simultaneous during the normal period of the loading of the tectonic stress, and the positive simultaneous correlation is disturbed for several years before a large earthquake of the region. This hypothesis is in harmony with the conclusion of ZOBACK AND ZOBACK (2002) about the spatial variations of seismicity from a global survey of the tectonic stresses that the tectonically stable region is stable because of the low rate of deformation in its ductile part, and the active region is active because of the high rate of this deformation.

Testing the above hypothesis with available observations is an uneasy statistical problem. First, the lithosphere is not accessible for direct measurements, and the technique for estimating Q^{-1} (JIN AND AKI, 1993; AKI, 1996) involves some arbitrary choices (free parameters). Second, in some cases the number of earthquakes with magnitude around M_c is small. For instance, $4.0 \le M \le 4.5$ suggested for central California in JIN AND AKI (1993) corresponds to less than 10 earthquakes per year, which is indeed challenging for studying processes with characteristic time scale of few years. Third, smoothing the raw observations, inevitable with high noise-to-signal ratio, brings in new adjustable numerical parameters, increasing the danger of self-deception (by possible data overfitting). It is important to emphasize that due to the intrinsically sparse and indirect character of the relevant data the above problems can hardly be resolved by increasing the quality of measurements or improving their spatio-temporal resolution. In such a situation the role of specifically tailored statistical methods can not be overestimated.

We present below (Sect. 3) a formal statistical technique for detecting temporal (un)correlations between time series observed at irregular, not coincident time grids. The technique is based on recently introduced Multiscale Trend Analysis (MTA) of time series (ZALIAPIN et al., 2003). MTA detects the most prominent trends (local linear approximations) of a time series $X(t)$ at different scales thus forming a hierarchy of trends, M_X. This hierarchy is then used for quantitative analysis. Our approach consists of two stages: First, we use MTA to detect prominent trends of $N(t)$ and $Q^{-1}(t)$. Second, we use basic characteristics of these trends (duration and direction) to quantify correlations between the time series. Results of our analysis clearly confirm previous findings by AKI (1996, 2003), JIN AND AKI (1989, 1993), and JIN et al. (2003). At the same time the proposed approach has significant advantages over the conventional statistical techniques (see Sect. 4.)

The paper is organized as follows. Section 2 describes the analyzed data and defines the functions $Q^{-1}(t)$ and $N(t)$. Section 3 introduces statistical method for quantifying (un)correlations between Q^{-1} and N, and applies it to the data. Results are discussed in Sect. 4.

2 Data

The study area is a circle centered at the station Mount Hamilton (121°38′30″E, 37°20′30″N), California, with radius of 120 km. The seismograms and earthquake catalog used for this study cover the time period from 1940 to 2003 (see Figure 1).

2.1 Coda Q^{-1} measurements

According to the single-back scattering model of seismic coda waves (Aki and Chouet, 1975), for a seismogram of a local earthquake the coda amplitude $A(f|t)$ for frequency f at lapse time t (measured from the origin time of the earthquake) can be expressed as

$$A(f|t) = A_0(f)t^{-\alpha}\exp\left(-\pi f Q^{-1}t\right), \tag{1}$$

where $A_0(f)$ is the source term, and $t^{-\alpha}$ represents the geometrical spreading for body waves ($\alpha = 1$) and for surface waves ($\alpha = 0.5$). Short period seismograms recorded at Mt. Hamilton for earthquakes occurred within 60 km around the station are used to estimate coda Q^{-1}. For the time period 1940-1990, the paper recordings of the Wood-Anderson and Benioff seismographs were used; the amplitude response of these instruments is peaked around 1.5 Hz. Each seismogram was first enveloped and then digitized in a sampling rate of 20/second. For the time period 1989-2003, the digital seismograms are used: they were filtered by a band-pass filter of 0.5-3.5 Hz in order to keep the consistence with the paper recording measurements. The coda amplitude $A(f|t)$ is measured using a 5-sec sliding time window (with 2.5 sec overlap) started at the lapse time twice of the S-travel time and ended at the signal twice the noise-level or 80 s, whichever comes first; this corresponds to, approximately, 120 km coda sampling region around the station, laterally and vertically, according to the single-back scattering model (Aki and Chouet, 1975).

The relatively large variations of coda Q^{-1} are inherent for its measurement and can only be reduced by averaging over many observations (JIN AND AKI, 1989, 1993). The coda Q^{-1} for each individual seismogram are averaged over 11 successive earthquakes with the overlap of 5 events. The time of each averaged measurement is attributed to the middle of the origin times of the corresponding 11 events. The coda $Q^{-1}(t)$ is shown in Fig. 2a.

2.2 Seismic activity

The ANSS earthquake catalog (available at http:// quake/ geo.berkeley.edu/ anss/ catalog-search.html) is used to study the seismicity in a region 120 km around the station Mount Hamilton. As suggested by JIN AND AKI (1993), the dynamics of seismicity is described by the time series $N(t)$ defined as the fractional frequency of earthquakes with magnitude $4.0 \leq M \leq 4.5$ among 100 consecutive earthquakes with $M \geq 3.0$. The value of $N(t)$ is attributed to the middle of the origin times of the corresponding 100 events. Figure 2b shows the time series $N(t)$ for 1940-2003.

3 Multiscale Trend Analysis

In this section we compare the dynamics of seismicity expressed by $N(t)$ with temporal change in the coda $Q^{-1}(t)$ (Fig. 2). First, we quantify the overall correlation between the two time series (Sect. 3.1); then detect periods when the correlation is destroyed (Sect. 3.2).

The correlation is analyzed in two ways: by comparing a) the slopes of the series' local trends (a coarse analog of the first derivative) and b) the slope changes (a coarse analog of the second derivative).

3.1 Detecting correlation between N and Q^{-1}

Here we quantify correlation between $N(t)$ and $Q^{-1}(t)$. The correlation is defined trough simultaneous rises and falls observed within the time series at different time scales. To formalize this, we use the MTA correlation defined in (Zaliapin et al., 2003): First, we construct an MTA tree M_N for $N(t)$ (see Fig. 3.) Each level l of this tree corresponds to a piece-wise linear approximation $L_l^N(t)$ of $N(t)$. The larger the level index l, the more detailed the corresponding approximation. Importantly for our subsequent analysis, each level l of M_N generates a partition P_l of the observational time interval into a set of n_l non-overlapping subintervals p_i^l, $i = 1, \ldots, n_l$.

3.1.1 Correlation using trend slopes

We denote by s_i^N $\left(s_i^Q\right)$, $i = 1, \ldots, n_l$ the slopes of the best linear approximations of $N(t)$ $(Q^{-1}(t))$ at the subintervals p_i^l of P_l. To avoid heavy notation we do not mark the dependence of the slopes on the level index l. Note that we use interval partitions P_l associated with $N(t)$ to determine the trend properties of both N and Q^{-1}. For robustness, the slopes s_i are coarsely binned defining new variables b_i:

$$b_i = \begin{cases} -1, & s_i \leq -s_0 \\ 0, & -s_0 < s_i < s_0 \\ 1, & s_i \geq s_0 \end{cases} \tag{2}$$

Measuring the correlation, we use the intuitively transparent idea that if N and Q^{-1} are correlated, their trend directions ("up" vs. "down") should match within the same time periods. It means that the series b_i calculated for $N(t)$ and $Q^{-1}(t)$ should be correlated in the usual sense (recall that these series now are calculated at the same time grid determined by P_l.) Formally, we define the correlation coefficient $r_l\,(N, Q^{-1})$ corresponding to level l of the decomposition M_N as follows:

$$r_l = \sum_{i=1}^{n_l} b_i^N b_i^Q \Delta_i. \tag{3}$$

Here the upper index denotes the time series whose slopes are binned by (2); Δ_i is the length of i-th subinterval of partition P_l. One can similarly define correlation r_{lk} corresponding to different levels of M_N: b_l^N would correspond to the level l while b_k^Q to the level k (see ZALIAPIN et al. (2003) for formal definitions.)

Figure 4a shows a correlation diagram: $r_{lk}\,(N, Q^{-1})$ as a function of levels $l, k = 1, \ldots, 28$ of the decomposition M_N. We see three domains of high correlation: at $l, k = 3$; $5 \leq l, k \leq 10$; and $12 \leq l, k \leq 16$. Figure 4b shows the same correlation as a function of the time scale defined as the average length of partition subintervals at a given level; such representation is more transparent physically. One observes three domains of high correlation: one corresponds to large time scales (tens of years), another to intermediate scales (years), and the last to short scales (months). The largest correlations correspond to the diagonal of the diagram, $r_l \equiv r_{ll}$, where the same partitions are used for both the time series. Solid line in Fig. 5 shows the correlation r_l, $l = 1, \ldots, 28$ calculated along the diagonal. The most interesting for our problem is the correlation peak, observed at level $l = 6$: $r_6 = 0.94$. The characteristic time scale for this correlation is 5.1 years, comparable with the characteristic time scales of the processes responsible for premonitory uncorrelations of Q^{-1} and N suggested in (AKI, 1996, 2003; JIN et al., 2003). Figure 6 shows both the time series together with the partition P_6 at 6-th level of the decomposition M_N. The corresponding trend directions b_6 (calculated with $s_0 = 0$) are depicted by color code. This figure illustrates the essence of the MTA correlation technique: we compare time series at a specific time scale, a priori unknown, eliminating "structural leftovers" insignificant for our specific problem. When this is done one sees indeed that the correspondence between the two time series is substantial, all the trend directions are matched except a discrepancy during 1993 to 1995 within a 22-months subinterval.

3.1.2 Correlation using slope differences

The same analysis as in the previous section can be done with respect to the slope differences, a counterpart of the second derivative, by analyzing the differences $d_i = s_{i+1} - s_i$ between consecutive slopes. Again, the binning (2) is applied and formula similar to (3) defines the correlation r'_l. The values of r'_l, $l = 1, \ldots, 28$ are shown in Fig.

5 by the dotted line: the slope difference correlation r' is similar to r.

3.2 Detecting uncorrelated periods

In this section we detect uncorrelated periods in dynamics of $N(t)$ and $Q^{-1}(t)$. As in the previous section, we compare different characteristics of their trends within the partition subintervals resulting from the MTA decomposition M_N.

Figure 7 shows time periods when trends b_i (upper panel) or trend differences d_i (lower panel) of $N(t)$ and $Q^{-1}(t)$ mismatch. We show only the levels $l = 4 - 11$ which cover the temporal scales 2-8 years (see Sect. 3.1, Fig. 4.) Most of the time the coarse trends (trend differences) are the same (white space in the figure.) Both the characteristics diverge (dark intervals) during the period 1980-2000. This is seen at all the levels (i.e. time scales) considered. From Fig. 7 it can be conjectured that larger temporal scales become uncorrelated first and are followed in a couple of years by uncorrelations at consecutively smaller scales.

Figure 8 further illustrates the perfect trend correlation that remains even at the detailed time resolution, 25 months on average. We use here the binned trend slopes b_i for N and Q^{-1} at level $l = 12$, which is not shown in Fig. 7. The trend matching extends even to a very specific trend pattern observed during the middle 80-s: a sequence of 5 trends with three upward trends separated by two very short downward ones. Interestingly, this sequence immediately preceded the first mismatched interval in 40 years. This interval was followed within a year by the 1989 Loma Prieta earthquake, $M = 7.0$, the largest within the region considered.

3.3 Summary of results

Here we sum up the observations made in the above two sections:

- $N(t)$ and $Q^{-1}(t)$ are strongly correlated during the period 1940-2003. The positive correlation is formally established at a wide range of temporal scales: from months to 30 years. The positive correlation is strong (the correlation coefficient (3) is above 0.5) for the time scales from 1 to 6 years (Figs. 4, 5.) The maximal correlation ($r_3 = 1$) is observed at the time scale of tens of years which corresponds to the global processes at the brittle-ductile transition zone caused by the plate-driving forces. The second correlation peak ($r_6 = 0.94$) is observed at the temporal scale about 5 years, matching the time scale suggested for the local brittle-ductile interactions in JIN et al., (2003); AKI, (2003). Recall, that the characteristic temporal scale is defined as the average duration of codirected (simultaneous "ups" or "downs") trends within the time series.

- $N(t)$ and $Q^{-1}(t)$ become uncorrelated during the period 1988-2000. The uncorrelation is observed at temporal scales from 2 to 12 years; it tends to appear earlier at larger time scales (longer trends) and is followed by uncorrelation at smaller scales (shorter trends). Notably, the uncorrelation is only observed prior to and around the time of the largest earthquake within the time-space considered (Loma Prieta, 1989, $M = 7.0$.)

4 Discussion

We presented a statistical technique aimed at detecting temporal (un)correlations between time series observed at irregular not coincident time grids. The technique is based on recently introduced Multiscale Trend Analysis of time series (ZALIAPIN et al., 2003), which uses coarse and robust representation of a series in terms of its observed trends (local linear approximations). Temporal correlation between two series is defined via correspondence of their trends (see Sect. 3.) Such a definition takes advantage of intuitively clear dynamical features of the analyzed processes (activation, relaxation, and quiescence); at the same time it is coarse enough in order not to overaverage the possible coupling effect.

We applied our technique to detecting correlations between the dynamics of the ductile and brittle layers of the Earth lithosphere. Our analysis confirms the observations made previously by JIN AND AKI (1989, 1993) and AKI (1996) about (un)correlations between coda Q^{-1} and fractional rate $N(M_c)$ of the occurrence of earthquakes with magnitude about M_c; it also confirms the recently formulated "Brittle-Ductile interaction hypothesis" (AKI, 2003; JIN et al., 2003). The introduced technique has the following advantages before the conventional correlation analysis:

- It allows one to work directly with not coincident time grids without preliminary resampling the data.
- Robustness: The correlation is defined via the stable objects — trends — rather

than noisy individual observations.

- Temporal scaling: The suggested technique quantifies the (un)correlations at different temporal scales. This allows one a) to detect the temporal scale responsible for (un)correlation, and b) to take into account possible variations in the time scale of the studied phenomena.

A good illustration of these advantages is comparison of the correlation (3) (see Fig. 4, 5) with the standard correlation coefficient R between Q^{-1} and N. Resampling of Q^{-1} and N at the time grid consisting of the observational points from both the time series leads to $R = 0.36$, which hardly hints at the strong coupling between the series! More than that, imagine an observer who calculates $R(t)$ using all the data collected by the time t: he would observe the decreasing correlation line shown in Fig. 9. Obviously, this line rather contradicts the intuitively transparent observation that the time series are uniformly correlated during 1940-1988 (cf. Fig. 6.)

Earthquakes are very difficult objects for scientific studies due to, mainly, two reasons: First, they occur in the deep of the Earth, and so far we are not able to make any direct observations and/or measurements at even close to the source areas. Second, earthquakes are rare events so the data accumulating process is relatively long. Therefore, insufficient data quality is an intrinsic obstacle in this field. It is of high importance to develop data-and problem-adaptive statistic methods to cope with this obstacle. The technique presented here is an example of such adaptive approach; it can help in deeper understanding the processes at the ductile-brittle boundary of the Earth lithosphere.

It is also of general interest for detecting correlations between non-stationary processes observed at irregular not coincident time grids.

Figure captions

Figure 1. Seismicity of California. The Mount Hamilton station is shown by a star. The region considered in the study is shown by a circle. Filled dots show epicenters of earthquakes with magnitude $M \geq 4$; their size is proportional to the magnitude.

Figure 2. Time series reflecting the dynamics of the ductile ($Q^{-1}(t)$, panel a) and brittle ($N(t)$, panel b) layers. See definitions in Sect. 2. Both the time series exhibit similar fluctuations at the time scale of 5-10 years during 1940-1988. After that the correlation rather vanishes. Quantifying this (un)correlations is the goal of our study.

Figure 3. MTA tree M_N for the time series $N(t)$. Each panel corresponds to a separate tree level, whose index l is indicated to the left. Each level l defines a piece-wise linear approximation $L_l(t)$ (solid lines) of $N(t)$ (dashed lines). Color code depicts directions of the local trend within $N(t)$: dark for "ups" and light for "downs". Detailness of the approximations increases with the level l: at each consecutive level $l+1$ MTA tries to single out the most prominent variations of $N(t)$ around the previous approximation $L_l(t)$ and leave less significant "structural leftovers" for the deeper levels of the decomposition.

Figure 4. Correlation diagram $r_{lk}\,(N, Q^{-1})$ based on the trend correlation (3.) The value r_{lk} is the correlation between $N(t)$ and $Q^{-1}(t)$ considered at the levels l and k of M_N correspondingly. The correlation is shown as a function of levels (panel a) and time scales (panel b.) The three separated domains of high correlation are clearly seen in both the panels. We concentrate on the middle one, $5 \leq l, k \leq 10$; its time scale of years is

comparable with the time scale previously reported for the ductile-brittle correlations.

Figure 5. Diagonal section of the correlation diagram of Fig. 4. Levels are marked in parentheses. Dotted line shows correlations estimated using slope differences (see Sect. 3.1.2.)

Figure 6. MTA decompositions $L_6^N(t)$ (panel a) and $L_6^Q(t)$ (panel b) corresponding to the levels of maximal correlation $l, k = 6$ in Figs. 4, 5. Color code is the same as in Fig. 3. Note that within a 60-year time interval considered there is only one, 22 months long, discrepancy in trend directions (around 1993).

Figure 7. Intervals of uncorrelations within time series $N(t)$ and $Q^{-1}(t)$. Uncorrelation is defined as a mismatched trend direction (panel a) or slope difference (panel b) within piece-wise linear approximations $L_l^N(t)$ and $L_l^Q(t)$ at different levels l of MTA decomposition M_N (see Fig. 3.) See Sect. 3.2 for details; s_0 is a 20% quantile of $|s_i|$.

Figure 8. MTA decompositions $L_{12}^N(t)$ (panel a) and $L_{12}^Q(t)$ (panel b). Color code is the same as in Fig. 3; white intervals correspond to the "zero" slopes, $b_i = 0$ (s_0 is a 20% quantile of $|s_i|$); we do not consider them in the analysis. Note the strong correspondence of the trend directions ("up" vs. "up", "down" vs. "down") during 1940-1988, and of the very specific trend pattern during 1982-1988. The first discrepancy is observed in 1988, a year prior to the 1989 Loma Prieta earthquake, M=7.0.

Figure 9. Standard correlation R between N and Q^{-1} calculated at intervals $[1940, t]$, $t \in [1945, 2003]$.

References

[1] Chouet, B. (1979). *Temporal variation in the attenuation of earthquake coda near Stone Canyon, California*, Geophis. Res. Lett., *6*, 143-146.

[2] Aki, K. (1985), *Theory of earthquake prediction with special reference to monitoring of the quality factor of lithosphere by the coda method,* Earthquake Pred. Res., *3*, 219-230.

[3] Jin, A. and Aki, K. (1986), *Temporal change in coda-Q before the Tangshan earthquake of 1976 and the Haicheng earthquake of 1975,* J. Geophys. Res., *91*, 665-673.

[4] Robinson, R. (1987), *Temporal variations in coda duration of local earthquakes in the Wellington region, New-Zealand,* Pure Appl. Geophys., *125*, 579-596.

[5] Tsukuda, T. (1988), *Coda-Q before and after the 1983 Misasa earthquake of M-6.2, Tottori prefecture, Japan,* Pure Appl. Geophys., *128*, 261-279.

[6] Sato, H. (1988), *Temporal change in scattering and attenuation associated with the earthquake occurrence — a review of recent studies on coda waves,* Pure Appl. Geophys., *126*, 465-497.

[7] Jin, A, and Aki, K. (1989), *Spatial and temporal correlation between coda* Q^{-1} *and seismicity and its physical mechanism,* J. Geophys. Res, *94*, 14041-14059.

[8] Jin, A, and Aki, K. (1989), *Temporal correlation between coda Q^{-1} and seismicity — evidence for a structural unit in the brittle-ductile transition zone,* J. Geodyn., *17*, 95-120.

[9] Aki, K. (1996), *Scale dependence in earthquake phenomena and its relevance to earthquake prediction,* P. Natl. Acad. Sci. USA, *93*, 3740-3747.

[10] Jin, A., Aki, K., Liu Z., and Keilis-Borok, V. (2003), *Brittle-Ductile Interaction Hypothesis for Earthquake Loading,* Hagiwara Symposium, XXIII General Assembly of IUGG, 2003, Sapporo, Japan.

[11] Aki, K. (2003), *A new view of earthquake and volcano precursors,* to be submitted to the Proceedings of the Hagiwara symposium, Earth, Planets and Space.

[12] Aki, K. (2003a), *A new view of precursory phenomena for volcanic eruptions and earthquake occurrences,* Abstract (#JSS01-016703-1), Hagiwara Symposium, XXIII General Assembly of IUGG, 2003, Sapporo, Japan.

[13] Zoback, M. D., and Zoback, M. L. (2002), *State of stress in the Earth's lithosphere,* in *International Handbook of Earthquake and Engineering Seismology*, Academic Press, Amsterdam, 559-568.

[14] Zaliapin, I., Gabrielov, A., and Keilis-Borok, V. (2003), *Multiscale Trend Analysis.* Submitted to Fractals. arXiv:physics/0305013v2.

(http://www.arxiv.org/abs/physics/0305013)

[15] AKI, K., and CHOUET, B. (1975), *Origin of Coda Waves: Source, Attenuation and Scattering Effects,* J. Geophys. Res., *80*, 3322-3342.

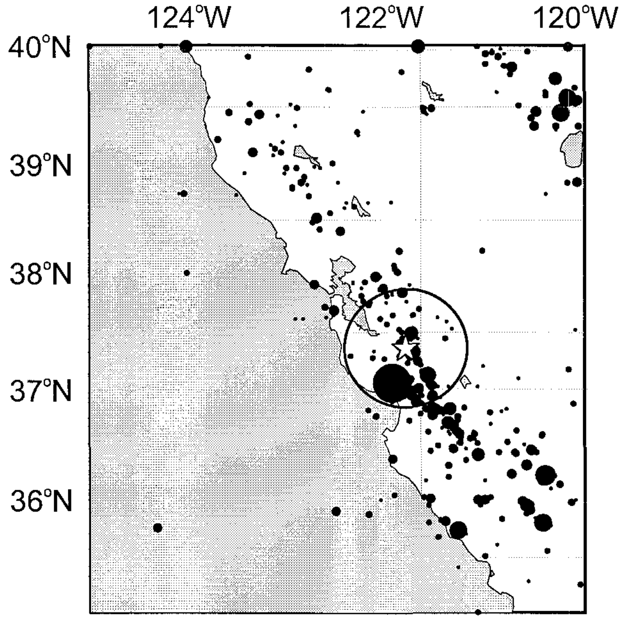

Fig. 1

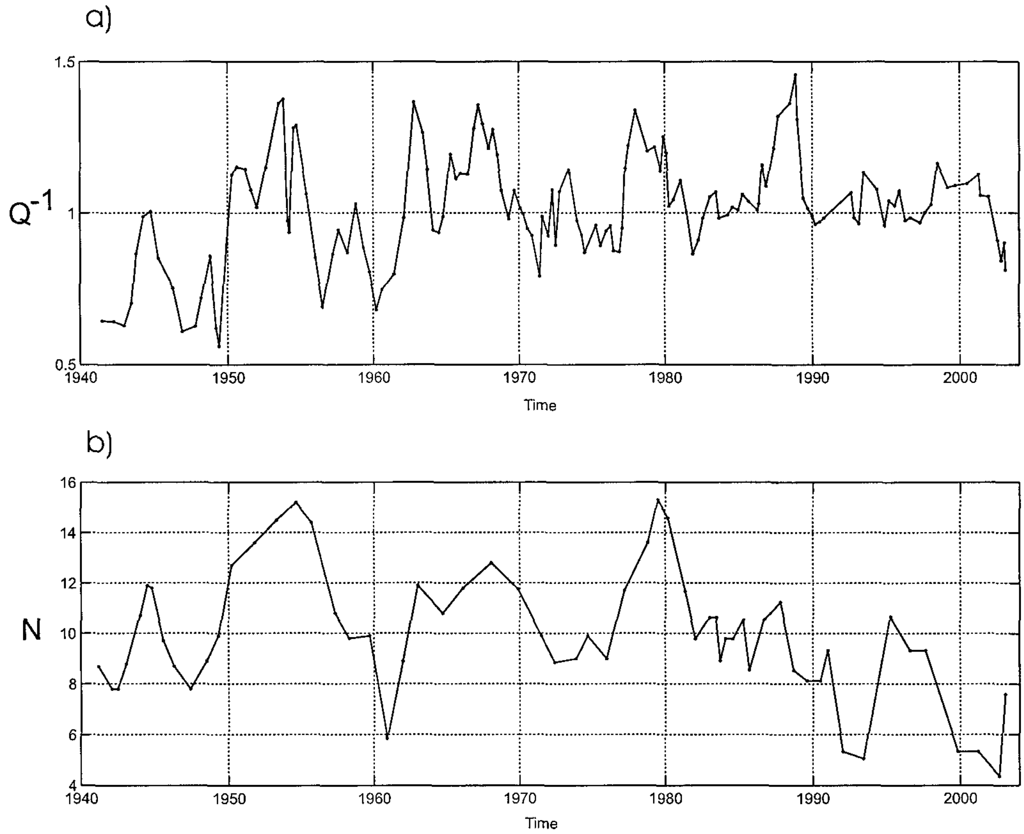
a)
1.5
1
0.5
Q-1
1940
1950
1960
1970
1980
1990
2000
Time
b)
16
14
12
10
8
6
4
N
1940
1950
1960
1970
1980
1990
2000
Time

Fig. 2

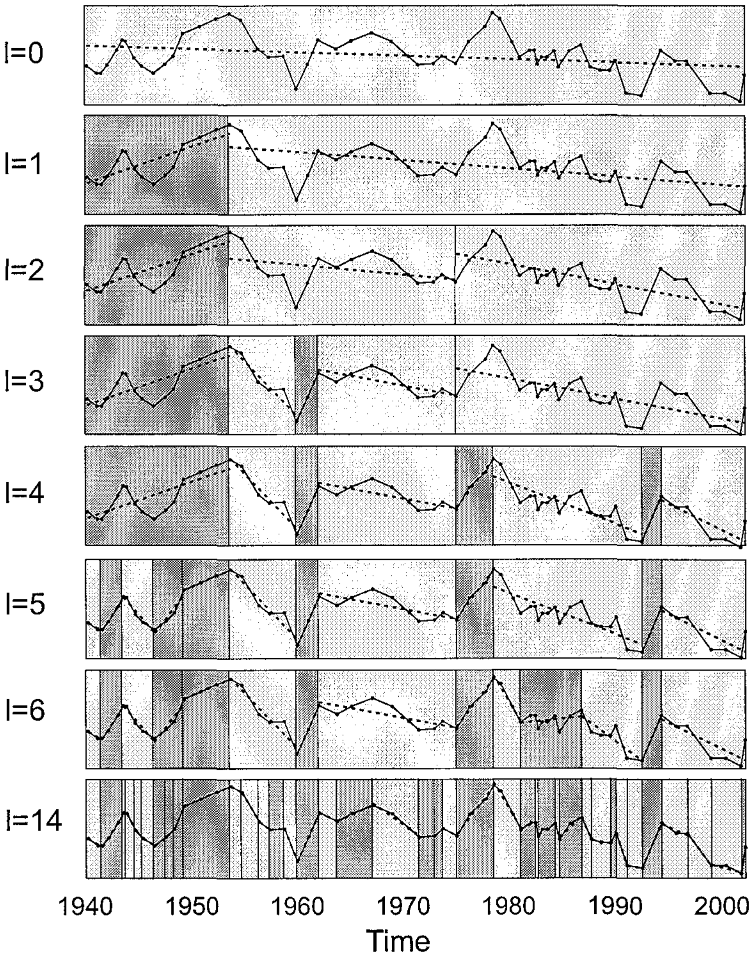

Fig. 3

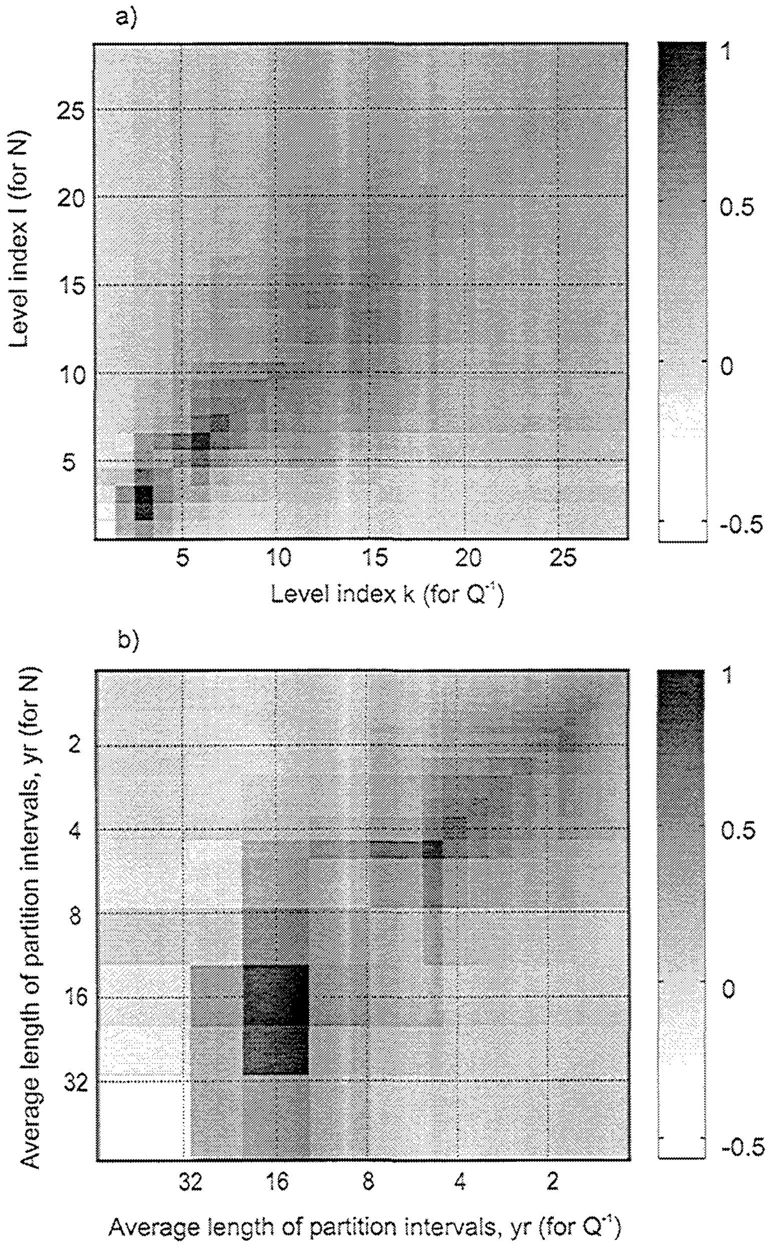

a)
25
20
15
10
5
Level index l (for N)
5
10
15
20
25
Level index k (for Q-1)
1
0.5
0
-0.5
b)
2
4
8
16
32
Average length of partition intervals, yr (for N)
32
16
8
4
2
Average length of partition intervals, yr (for Q-1)
1
0.5
0
-0.5

Fig. 4

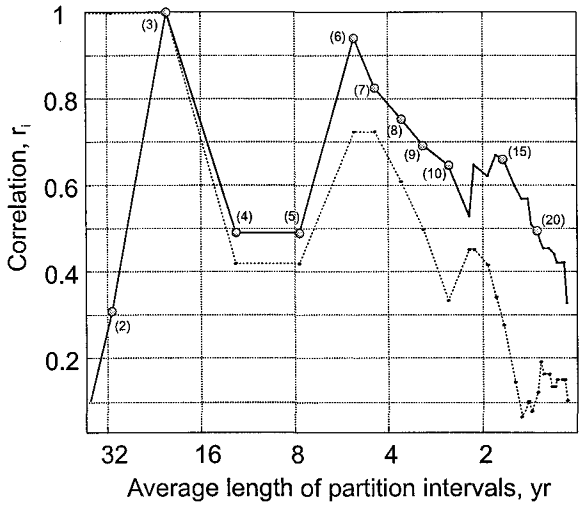
1
0.8
0.6
0.4
0.2
Correlation, r_i
(3)
(6)
(7)
(8)
(9)
(10)
(15)
(4)
(5)
(20)
(2)
32
16
8
4
2
Average length of partition intervals, yr

Fig. 5

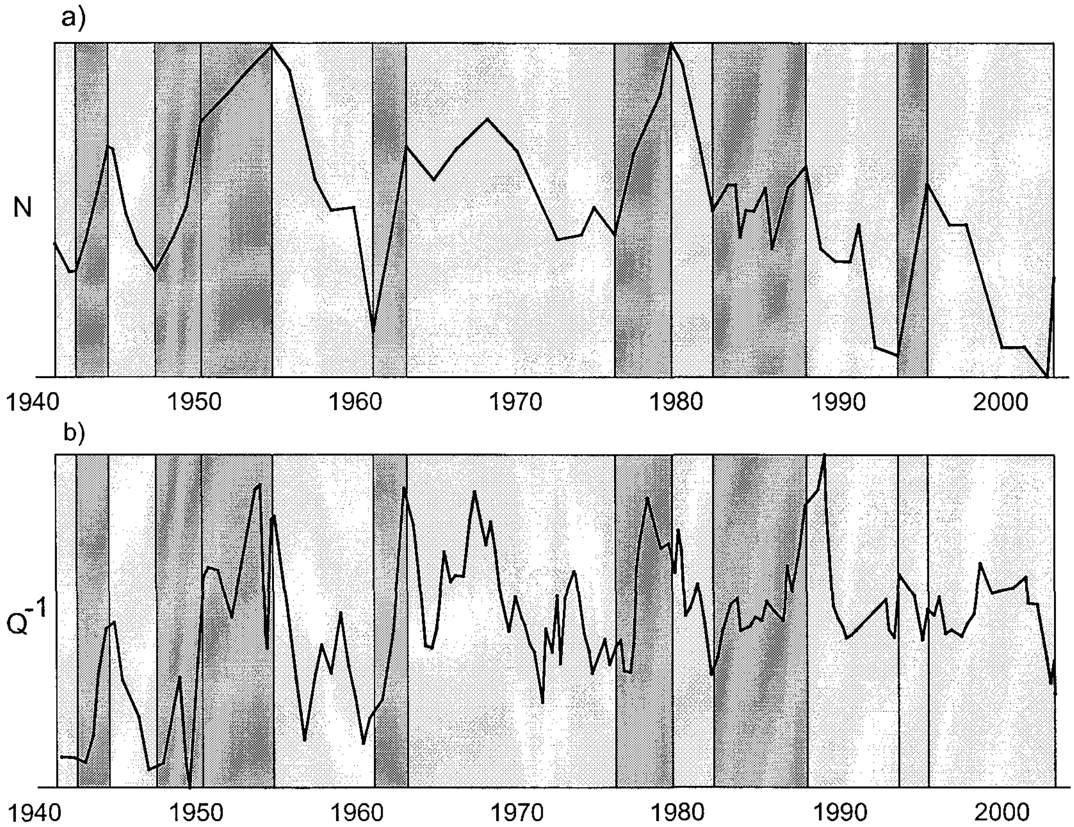
a)
N
1940
1950
1960
1970
1980
1990
2000
b)
Q^{-1}
1940
1950
1960
1970
1980
1990
2000

Fig. 6

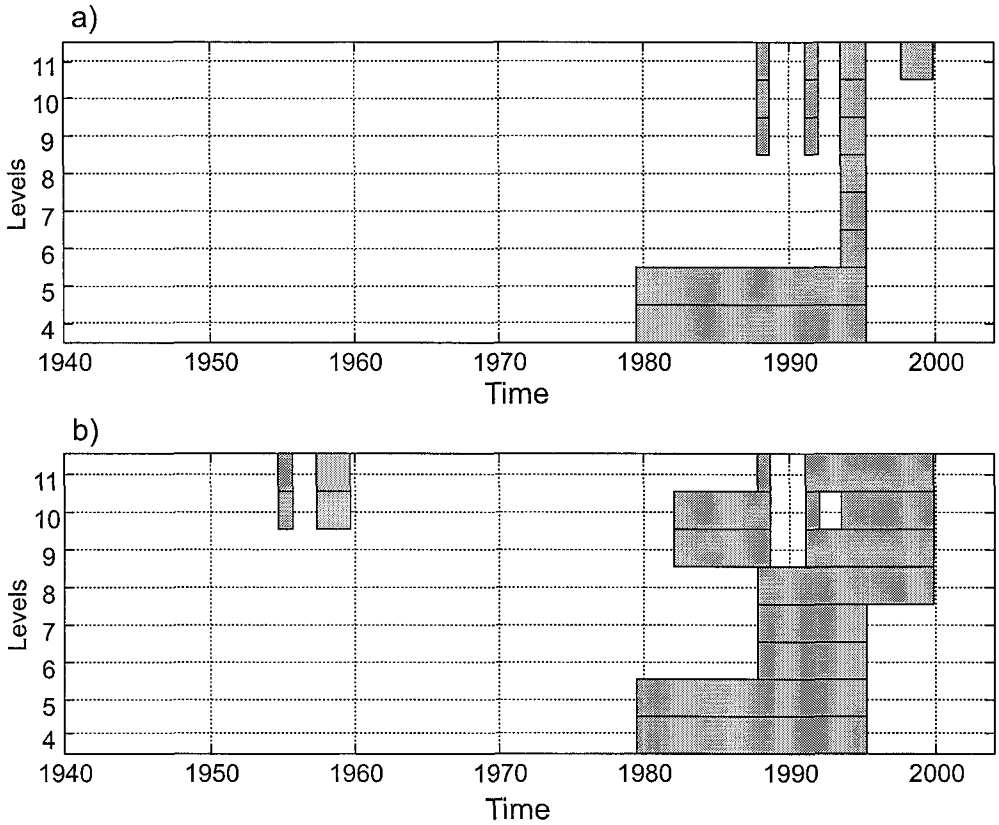
a)
Levels
11
10
9
8
7
6
5
4
1940
1950
1960
1970
1980
1990
2000
Time
b)
Levels
11
10
9
8
7
6
5
4
1940
1950
1960
1970
1980
1990
2000
Time

Fig. 7

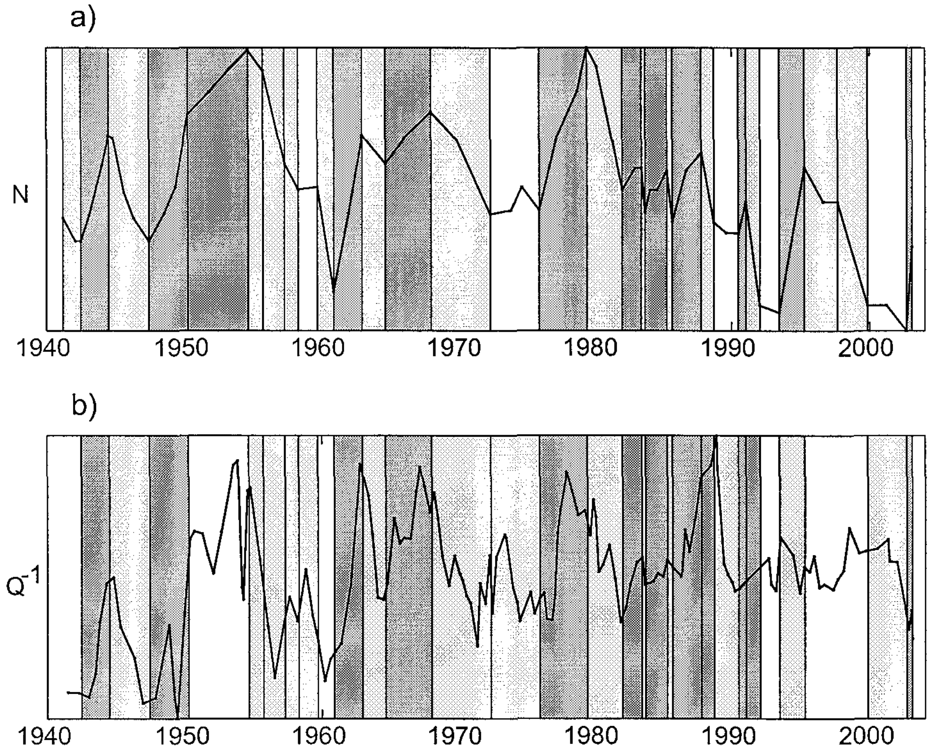

a)
N
1940
1950
1960
1970
1980
1990
2000
b)
Q-1
1940
1950
1960
1970
1980
1990
2000

Fig. 8

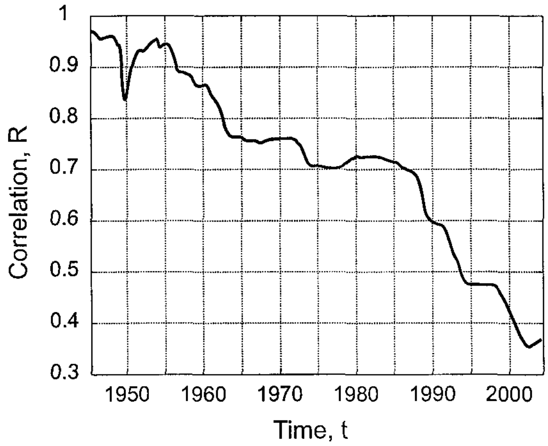
1
0.9
0.8
0.7
0.6
0.5
0.4
0.3
Correlation, R
1950
1960
1970
1980
1990
2000
Time, t

Fig. 9